The domain switching and structural characteristics of PLZT bulk ceramics and thin films chemically prepared from the same acetate precursor solutions

D. E. DAUSCH*, G. H. HAERTLING
Gilbert C. Robinson Department of Ceramic Engineering, Clemson University, Clemson, SC 29634, USA

Lead lanthanum zirconate titanate (PLZT) ferroelectrics were produced in bulk ceramic and thin-film form from the same acetate precursor solutions in order to compare their electrical and physical properties. Bulk ceramics were hot pressed from chemically coprecipitated powders, and thin films were fabricated by spin coating on silver foil and platinum-coated silicon wafer substrates. A number of PLZT compositions were investigated, including ferroelectric memory materials near the morphotropic phase boundary with 2% La, memory and slim-loop ferroelectric *x*/65/35 (La/Zr/Ti) compositions with up to 12% La, as well as some antiferroelectric thin-film materials. Internal film stress from thermal expansion mismatch between films and substrates was found to contribute to differences in electrical properties and Curie temperatures between the thin film and bulk materials, as were interface layers between the films and substrates, mechanical clamping from the substrates and grain size.

1. Introduction

The wide range of unique properties of lead lanthanum zirconate titanate (PLZT) ferroelectric materials, including superior piezoelectric, dielectric, pyroelectric, ferroelectric, electrostrictive and electrooptic properties, has led to useful electronic ceramic devices such as piezoelectric actuators, multilayer capacitors, electro-optic shutters and pyroelectric sensors [1, 2]. Traditionally produced in bulk ceramic form, the applicability of PLZT materials was increased and their ease of processing was improved as more recent developments in thin-film technology were utilized. Memories for integrated circuits [3–5] and thin-film electro-optic devices [5, 6] became plausible since thin films possessed lower operating voltage, higher access speed and compatibility with semiconductor integrated circuits compared with traditional bulk ceramics. With thin-film fabrication, especially sol–gel and metallo-organic decomposition (MOD) processes, reduced sintering temperatures and processing times, more reproducible thickness and compositional control, lower cost, fabrication simplicity and increased variability in sample geometry and size were realized for ferroelectric materials [5, 7, 8].

Despite the advantages of thin-film materials, thin-film ferroelectric response is often diminished compared with typical bulk ceramic properties; for example, more difficulty in domain switching resulting in less square, more poorly developed hysteresis loops. In order to understand more fully and to optimize thin-film ferroelectric behaviour, a comparison is necessary to bulk ferroelectric phenomena. Direct correlation between the bulk and thin-film materials is difficult because the precursors and processing techniques of each are typically so dissimilar; however, a study is presented here that diminishes this disparity. This investigation of PLZT bulk ceramics hot pressed from chemically coprecipitated powder and thin films spin coated on silver foil and platinum-coated silicon wafer substrates which were produced from the same acetate precursor solutions, allows for a close comparison of bulk and thin-film ferroelectrics by minimizing or eliminating differences in the processing of these materials induced by batching variations, precursor impurities and differences in mixing, reactivity and chemical composition of the starting precursor materials. The dielectric and hysteresis properties, as well as the Curie temperatures, crystallinity and microstructures were observed. Internal stress, interface layer and grain-size effects on thin-film properties were considered. A knowledge of ferroelectric thin-film behaviour in comparison with bulk ceramics should lead to an understanding of the similarities and differences in domain switching and structural characteristics between these materials, as well as the usefulness and limitations of thin-film devices.

* *Present address:* NASA Langley Research Center, Hampton, VA 23681, USA.

0022–2461 © *1996 Chapman & Hall*

2. Experimental procedure

2.1. Materials preparation

A combined batching system was developed to produce chemically prepared PLZT hot-pressed ceramics and spin-coated thin films using the same batch of water-soluble acetate precursors [9]. This combined batching procedure was used to produce spin-coating solution for thin films as well as coprecipitated powder for bulk ceramics from the same acetate formulation. The starting precursors included lead subacetate powder, lanthanum acetate, zirconium acetate and titanium acetyl acetonate solutions. For batching simplicity and accuracy, the lead subacetate was mixed into solution form with acetic acid and methanol to produce a lead acetate solution so that all of the acetate precursors were liquids. This ensured that the beginning acetate formulation was readily and completely mixed into solution. Incomplete mixing could produce compositional fluctuations between the resulting coprecipitated powder and spin-coating solution. This wet chemical batching process has reduced the possibility of batching variations between bulk and thin-film materials so that differences in their properties were not a result of these variations.

After initial acetate formulation, the stock solution was separated for coprecipitation and spin coating. Coprecipitation occurred in a high-speed blender with the addition of oxalic acid and methanol to the acetates. The solution was then vacuum dried to produce a solid, friable cake which was crushed, calcined at 500 °C and ball milled to produce a fine PLZT oxide powder. Hot-pressing conditions for the powder were 1200 °C for 4 h at 14 MPa (2000 p.s.i.). To prepare samples for electrical measurement, the hot-pressed parts were sliced on a diamond saw and lapped to 0.5 mm (20 mil) thickness. Electroless nickel electrodes were plated on to the samples.

For thin-film production via spin coating, a small portion of solution was decanted from the acetate formulation and diluted with methanol at a 2:1 ratio by weight. Films were spun from the acetate solution on to silver foil and platinum-coated silicon wafer (Pt/Si) substrates using a photoresist spinner at 2000 r.p.m. for 15 s and then pyrolysed at 700 °C for 4 min in a Thermolyne box furnace. Repeating this process for ten layers produced a PLZT thin film approximately 0.9 μm thick. For measurement of electrical properties, 1 mm diameter copper electrodes were vacuum evaporated on to the surface of the films.

2.2. Thin-film and bulk ceramic analysis

Bulk and thin-film samples were analysed using several electrical and physical measurement techniques. Poled and virgin dielectric constants, K_{pol} and K_{vir}, and dissipation factors, $\tan\delta$, were measured on a Leader LCR meter at 1 kHz. The Curie temperatures, T_C, of bulk and thin-film samples were determined for several PLZT compositions and were indicated by maxima in the measured capacitance. Bulk samples were placed in a stirred oil bath and heated while taking capacitance measurements at 5 °C increments. Thin-film samples were heated in a Delta Design temperature controller. Capacitance was also measured from 100 Hz to 40 MHz using a Hewlett-Packard 4194A impedance analyser with a 100 mV a.c. signal.

Hysteresis loops of the bulk samples were measured using a Sawyer–Tower circuit with a d.c. applied voltage of ± 1400 V at approximately 1/4 Hz and were plotted with a Goerz Metrawatt X–Y plotter. Thin film hysteresis properties were customarily measured at 1 kHz with a 20–40 V a.c. signal using a Sawyer–Tower circuit and an oscilloscope readout. Additionally, in order more accurately to compare measurement of bulk and film hysteresis loops, some of the thin-film samples were measured using a low-voltage (± 30 to 50 V) d.c. looper at 1/4 Hz. X-ray diffraction patterns of thin films and bulk ceramics were obtained using a Scintag XDS 2000 diffractometer with CuK_α radiation. Film thicknesses were determined using a Tencor profilometer and Gaertner Scientific laser ellipsometer.

3. Results and discussion

Several compositions of hot-pressed bulk ceramics and spin-coated thin films were investigated near phase boundaries in the PLZT system. Morphotropic phase boundary (MPB) compositions, or those near the boundary between the lead zirconate-rich ferroelectric rhombohedral and lead titanate-rich ferroelectric tetragonal phases, consisted of 2/55/45 (La/Zr/Ti), 2/53/47 and 2/51/49, and these compositions exhibit ferroelectric memory behaviour with square hysteresis loops. Compositions near the slim-loop ferroelectric phase region, i.e. the region between the ferroelectric rhombohedral and paraelectric cubic phases, with 65/35 Zr/Ti ratios included those with 6%–12% La. These materials typically are memory materials from 6%–8% La, slim-loop ferroelectric materials which possess zero coercive field, E_C, and zero remanent polarization, P_R, with high induced polarization in the 9%–10% La range, and paraelectric cubic or non-ferroelectric with 12% La.

3.1. Crystallinity and microstructure

One significant influence on ferroelectric thin-film properties is internal stress resulting from thermal expansion mismatch between the film and substrate. Watanabe *et al.* [10] proposed that the mechanical stress present in PZT thin films caused by lattice or thermal expansion mismatch between the film and the substrate can cause differences in lattice constants between bulk and thin-film materials. It is known that PLZT has an intermediate coefficient of thermal expansion (CTE) of $5.4 \times 10^{-6}\,°C^{-1}$ compared to silver and silicon which possess CTEs of 19×10^{-6} and $2.6 \times 10^{-6}\,°C^{-1}$, respectively [1, 11, 12]. Hence, a two-dimensional compressive stress is imparted on PLZT thin films deposited on silver because the substrate contracts more than the film upon cooling to room temperature, and a two-dimensional tensile stress results in films deposited on silicon as the film tends to contract more than the silicon. As shown in

TABLE I X-ray diffraction d-spacings for a 2/55/45 bulk ceramic and thin films on silver and Pt/Si substrates. d-spacings are shown with the corresponding percentage change from bulk ceramic values

Plane	2Θ (deg)	d (bulk) (nm)	d (film on Ag) (nm)	d (film on Pt/Si) (nm)
(1 0 0)	22	0.4088	0.4131 (+1.05%)	0.4066 (−0.54%)
(1 1 0)	31	0.2879	0.2900 (+0.73%)	0.2869 (−0.35%)
(1 1 1)	38	0.2356	–[a,b]	0.2343 (−0.55%)
(0 0 2)	43.5	0.2076	–[b]	–[b]
(2 0 0)	44.5	0.2035	0.2060 (+1.23%)[a]	0.2030 (−0.25%)
(2 1 0)	50	0.1823	0.1839 (+0.88%)	–[b]
(2 1 1)	55	0.1663	0.1676 (+0.78%)	0.1660 (−0.18%)
(3 0 0)	65	0.1442	–[a,b]	0.1437 (−0.35%)

[a] Overlapped by silver substrate peak.
[b] Peak not detected.

Table I, PLZT thin film d-spacings increased as the crystal structure expanded normal to the silver substrate surface plane due to compressive stress; furthermore, residual strain from tensile stress parallel to the Pt/Si substrate plane resulted in a decrease in thin-film d-spacings normal to the substrate surface. The thin platinum electrode between the PLZT film and silicon substrate was assumed to incur a negligible effect on the tensile stress induced in the PLZT. In fact, X-ray diffraction revealed that the platinum layer, which has a CTE of $9 \times 10^{-6}\,°C^{-1}$ [11], also possessed an internal tensile stress as the platinum electrode d-spacings were found to decrease when constrained by the deposited PLZT thin film.

Despite the much greater disparity between the CTEs of PLZT and silver compared to PLZT and silicon, the shifts in d-spacings shown in Table I for the film on silver were typically only twice as large, i.e. an average increase of 0.9%, as for the film on silicon which exhibited an average decrease of 0.4%. This indicated that the more ductile silver substrate probably provided some degree of compressive stress relaxation through elastic deformation, while the more rigid silicon was not as forgiving. It should also be noted that three of the PLZT peaks were masked by silver substrate peaks. Peak splitting, which was observed in the (2 0 0)/(0 0 2) peak of the bulk 2/55/45 sample, was not observed in the constrained thin-film samples. As expected, scanning electron and optical micrographs of chemically etched 2/55/45 thin-film (on silver) and bulk ceramic samples, respectively, revealed that the thin film with grain size of roughly 0.5 μm exhibited a much finer microstructure than the bulk ceramic which possessed a grain size of approximately 2.5 μm. These micrographs were presented elsewhere [13].

3.2. Dielectric properties

The electrical properties are listed for bulk ceramics and thin films on silver in Table II including virgin and poled dielectric constants and dissipation factors for each, as well as coercive field and remanent polarization values from the a.c. and d.c. hysteresis loops, which will be discussed in the next section. The dielectric constants of the films on silver were generally 20%–30% lower than their bulk ceramic counterparts. Similar reduced dielectric constants have previously been reported to be due to several effects caused by the obvious differences between bulk and thin-film configurations, including small grain size of the thin films, film/substrate interface layers, mechanical clamping effects and voltage sensitivity of the dielectric measurement as a result of the high electric field created by the 1 V measuring signal applied to a 1 μm thin film [9]. The difference in dielectric properties found in the present results, however, was not as significant as reported in the literature. For films on Pt/Si, the dielectric constants were significantly lower than for bulk ceramics and films on silver. Dielectric constants near 800 were obtained for 2/55/45 on Pt/Si, while 8/65/35 and

TABLE II Dielectric and ferroelectric properties of PLZT hot-pressed bulk ceramics and spin-coated thin films on silver

		K_{pol}	Tan δ (pol)	K_{vir}	Tan δ (vir)	E_C (d.c.) (kV cm^{-1})	P_R (d.c.) (μC cm^{-2})	E_C (a.c.) (kV cm^{-1})	P_R (a.c.) (μC cm^{-2})
Bulk ceramics	2/55/45	1328	0.029	1293	0.033	8	46	–	–
	2/53/47	1885	0.025	1391	0.028	10	40	–	–
	2/51/49	1630	0.024	1234	0.034	16	33	–	–
	6/65/35	1355	0.036	1774	0.056	6	33	–	–
	7/65/35	2712	0.033	2479	0.036	5	31	–	–
	8/65/35	5700	0.055	4692	0.050	3	20	–	–
	9/65/35	5147	0.054	5007	0.050	0	0	–	–
	9.5/65/35	5658	0.048	5603	0.046	0	0	–	–
	10/65/35	5548	0.036	5538	0.033	0	0	–	–
Thin films	2/55/45	997	0.122	1228	0.133	27	34	43	32
	2/53/47	1265	0.132	1619	0.160	28	47	44	45
	2/51/49	972	0.122	1237	0.146	28	38	46	37
	6/65/35	1871	0.142	1995	0.141	14	21	28	25
	7/65/35	2499	0.170	2460	0.145	14	18	27	21
	8/65/35	3211	0.194	3172	0.176	11	15	22	19
	9/65/35	4221	0.195	4001	0.172	9	11	22	17
	9.5/65/35	4234	0.190	4092	0.164	7	8	19	18
	10/65/35	4157	0.193	4157	0.209	7	10	18	16

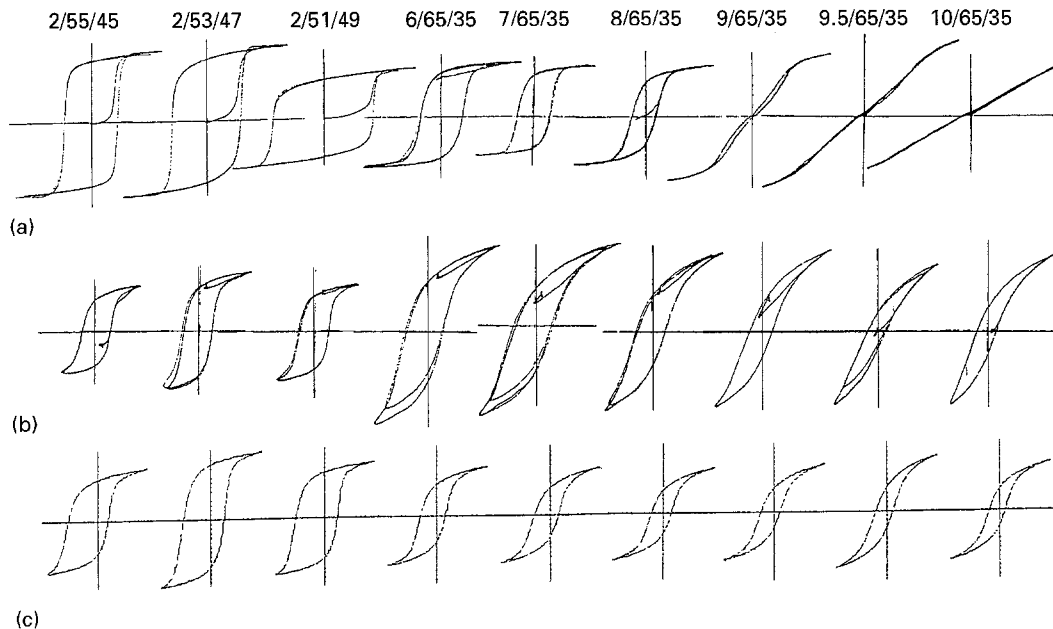

Figure 1 Polarization versus electric field hysteresis loops of PLZT bulk ceramics and thin films on silver. (a) Bulk ceramics, a.c.; (b) thin films, d.c.; (c) thin films, a.c.

9.5/65/35 compositions were much lower than expected, i.e. 545 and 575, respectively.

In comparing bulk 2% La samples to thin films on silver, some similarities and differences were noted. Unsurprisingly, both bulk and thin-film data showed maxima in K_{vir} and K_{pol} at the 2/53/47 composition, indicating the existence of the MPB at this composition; however, the position of this boundary for thin films seemed to be slightly different from that for the bulk samples. K_{pol} and K_{vir} for 2/51/49 thin films (972 and 1237) was essentially equal to that of 2/55/45 films (997 and 1228), while bulk 2/51/49 had a much greater poled dielectric constant (1630) than bulk 2/55/45 (1328). Because the dielectric constant was expected to peak at the MPB, this result suggested that this phase boundary in thin films was shifted slightly towards the lead zirconate end member in the phase diagram indicating enhanced stability of the tetragonal phase. Two-dimensional compressive stress in the thin-film samples probably enhanced tetragonal unit cell distortion (*c*-axis expansion normal to the substrate surface), while relatively stress-free bulk ceramics exhibited rhombohedral transformation at a lower Zr/Ti ratio (more towards the lead titanate end member).

For the *x*/65/35 compositions near the paraelectric phase boundary, the dielectric constant was expected to reach a maximum at this phase boundary which was previously reported at the 9/65/35 composition for bulk ferroelectrics produced via the mixed oxide process [14]. As expected, both film and bulk materials exhibited increasing dielectric constants with increasing lanthanum percentage. Bulk ceramic dielectric constants indicated a maximum for the paraelectric phase boundary at the 9.5/65/35 composition (5658 and 5603 for K_{pol} and K_{vir}) although an anomalously high K_{pol} of 5700 was observed for the 8/65/35 composition. This high K_{pol} may have been related to the boundary between the ferroelectric memory and slim-loop ferroelectric compositions, as shown by the hysteresis properties in the next section. For thin-film materials, a distinct peak in dielectric properties was not observed. K_{pol} and K_{vir} values in the range of 4000–4200 were exhibited by the *x*/65/35 thin films with 9%–10% La. In order to describe more fully the phase transition behaviour of these compositions, the Curie temperatures are presented in a later section. Despite differences in behaviour near phase boundaries, the dielectric properties of thin films on silver and bulk samples seemed to exhibit reasonable agreement as similar trends were observed.

3.3. Hysteresis properties

The ferroelectric properties calculated in Table II were obtained from the a.c. and d.c. *P–E* hysteresis loops shown in Fig. 1. As stated above in the discussion of dielectric properties, both bulk and thin-film 2% La materials exhibited a maximum in *K* indicating the existence of the MPB. A phase transition from rhombohedral to tetragonal symmetry as a function of composition was also evident in the hysteresis loops of these materials. In the bulk materials, a widening of the hysteresis loop with increased E_C of 16 kV cm^{-1} and decreased P_R of 33 μC cm^{-2} signalled a transition to the hard ferroelectric tetragonal phase in the 2/51/49 material. This phenomenon, however, did not occur in the thin-film samples on silver foil as evidence for the MPB was more subtle. The tetragonal phase was apparent in thin films with relatively squarer hysteresis loops for 2/51/49 than for the rhombohedral 2/55/45 film, as revealed by the slight increase in E_C and higher P_R for 2/51/49. A maximum in P_R in the 2/53/47 film indicated the occurrence of the MPB in both a.c. and d.c. hysteresis loops of the films. A number of investigators observed that thin films possess a higher coercivity and often contain a lower polarization remanence than bulk materials, owing to smaller

thin-film grain size, lack of complete film crystallization, film/substrate or film/electrode interaction, mechanical clamping or internal film stress [7, 9, 15–17]. Although the thin films presented here with 2% La had higher E_Cs, the P_Rs of these films were not necessarily lower than for bulk materials. In fact, 2/53/47 and 2/51/49 films had higher P_Rs (47 and 38 $\mu C\,cm^{-2}$) than bulk samples of the same composition (40 and 33 $\mu C\,cm^{-2}$). These thin films on silver did possess square hysteresis loops similar to the bulk; however, as with the dielectric behaviour, the hysteresis properties of the thin films were somewhat different across the phase boundary than the bulk ceramics. This was also the case for *x*/65/35 materials.

In PLZT bulk *x*/65/35 samples, the hysteresis loop characteristics occurred as expected. As anticipated, compositions with 6%, 7% and 8% La possessed ferroelectric memory loops, while the 9%, 9.5% and 10% La compositions exhibited slim-loop behaviour. For the memory materials, E_Cs were higher and P_Rs were lower for thin films than for bulk materials which was similar to previously reported results [9]. Although both bulk and thin-film memory materials experienced narrowing of their hysteresis loops with increasing lanthanum percentage, the bulk materials transformed to slim-loop ferroelectric at 9% La, while the thin films maintained ferroelectric memory hysteresis loops beyond 9% La with P_Rs ranging from 8–11 $\mu C\,cm^{-2}$ and E_Cs from 7–9 $kV\,cm^{-1}$. Research by Gu *et al.* [18] on quenched PLZT 9.5/65/35 ceramics showed that internal stresses induced in quenched samples can enhance polar-region ordering in these typically slim-loop materials. As a result, a more ferroelectric-like response with higher remanent polarizations was observed in quenched samples than in annealed samples that were cooled slowly. These findings could explain the memory behaviour observed in the 9, 9.5 and 10/65/35 thin films in this investigation. Residual compressive stress in the thin films on silver may have caused these films to retain ferroelectric memory hysteresis loops that were not observed in the bulk materials of the same compositions.

The a.c. hysteresis loops of thin films spin-coated on Pt/Si shown in Fig. 2 were much less square than those produced by either bulk samples or thin films on silver. E_Cs for the 2/55/45, 8/65/35 and 9.5/65/35 were 51, 55 and 43 $kV\,cm^{-1}$, respectively, while P_Rs were 10, 8 and 5 $\mu C\,cm^{-2}$ for these compositions. As with the thin films on silver, the 9.5/65/35 thin film on Pt/Si still exhibited ferroelectric memory behaviour as opposed to slim-loop characteristics. Films on Pt/Si, however, possessed much higher E_Cs and lower P_Rs indicating more difficulty of domain switching than films on silver of the same composition. The difference in hysteresis behaviour for these films on different substrates can be attributed to the type of stress imposed on the films by the underlying substrates. It has been proposed that the domains of films in compression will tend to align normal to the substrate surface plane or in the direction of the applied electric field; furthermore, films in tension will possess domains aligned parallel to the substrate surface or perpendicular to the electric field [12]. As a result, compressive stress enhances domain switching, resulting in ferroelectric behaviour similar to that of the bulk material with squarer hysteresis loops, while tensile stress impedes domain switching, resulting in more slanted loops. From the results in this investigation, it was evident that thin films deposited on silver foil under compressive stress had ferroelectric properties comparable with bulk ceramic materials; however, thin films deposited on Pt/Si under tensile stress possessed less square, more slanted hysteresis loops.

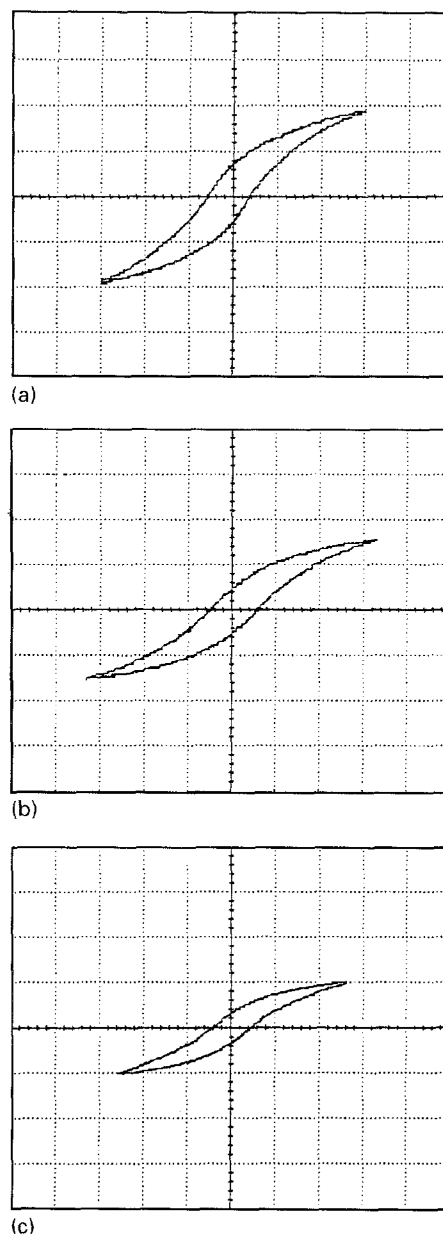

Figure 2 *P–E* hysteresis loops of PLZT (a) 2/55/45, (b) 8/65/35 and (c) 9.5/65/35 thin films deposited on Pt/Si. The scale for the *y*-axis (polarization) is 15 $\mu C\,cm^{-2}$ per division, and the *x*-axis (electric field) is 100 $kV\,cm^{-1}$ per division.

3.4. Curie temperature phase transitions

Because thin-film materials are often subjected to mechanical stress as they are cooled to room temperature, shifts in phase transition temperatures can occur [19–21]. Curie temperatures of bulk *x*/65/35 samples were determined by measurement of dielectric

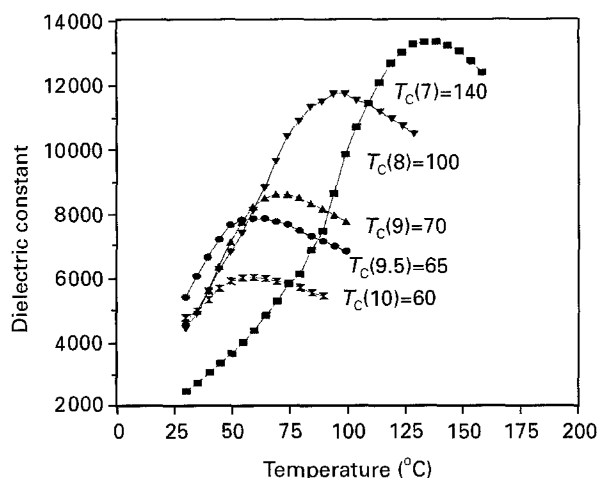

Figure 3 Curie temperature measurements of PLZT $x/65/35$ bulk ceramics: (■) 7/65/35, (▼) 8/65/35, (▲) 9/65/35, (●) 9.5/65/35, (⧗) 10/65/35.

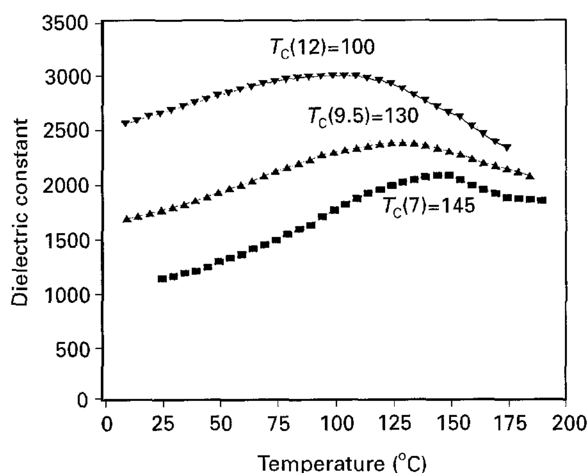

Figure 4 Curie temperature measurements of PLZT $x/65/35$ thin films deposited on silver: (■) 7/65/35, (▲) 9.5/65/35, (▼) 12/65/35.

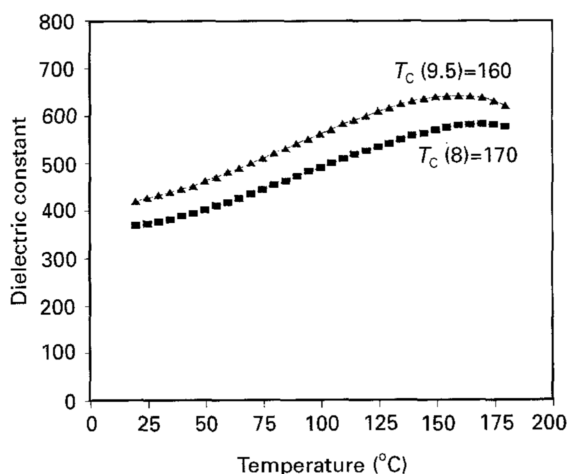

Figure 5 Curie temperature measurements of PLZT $x/65/35$ thin films deposited on Pt/Si: (■) 8/65/35, (▲) 9.5/65/35.

constants with increasing temperature and are shown in Fig. 3. The thin-film T_Cs shown in Fig. 4 for films on silver substrates were higher than those for the corresponding bulk compositions as were the T_Cs for films on Pt/Si shown in Fig. 5. Thin-film Curie temperatures exhibited a similar decrease with lanthanum percentage as shown in the bulk $x/65/35$; however, thin-film T_Cs occurred at much higher temperatures than the bulk. T_C increases for films on silver ranged from 5 °C for 7/65/35 to 65 °C for 9.5/65/35, while films on Pt/Si possessed increases as high as 95 °C for 9.5/65/35. As with their hysteresis properties, internal stress in the thin films allowed these materials to remain in the ferroelectric memory state at room temperature for 9%, 9.5%, 10% and even 12% La. Furthermore, the fact that Curie temperatures for these thin films remained well above room temperature was further evidence that indeed these films exhibited ferroelectric memory hysteresis behaviour because they were in the ferroelectric state at room temperature.

Another influence on thin-film Curie temperature shifts compared with bulk ceramics was grain size. Okazaki and Nagata [22] determined that T_Cs increased with decreasing grain size in hot-pressed PLZT ceramics. This shift in T_C, which was accompanied by a significant decrease in peak dielectric constant or flattening of the K versus temperature curve, was attributed to a space charge effect which locked in the ferroelectric polarization. As the grain size decreased, the surface area of the space charge layer surrounding the ferroelectric grains increased, and the ferroelectric to paraelectric phase transition was delayed to higher temperatures than normal as the ferroelectric polarization was shielded by this space charge. Okazaki and Nagata showed that a decrease in grain size from 2.5 μm to 0.5 μm, or bulk grain size compared to thin films for this research, corresponded to a greater than 20 °C increase in T_C and a decrease of at least 10 000 in peak dielectric constant for PLZT 8/65/35. In addition to increased T_Cs for the chemically prepared thin films in this investigation, a corresponding dramatic decrease in peak dielectric constant was observed similar to that reported by Okazaki and Nagata. This grain-size effect along with stresses induced by thermal expansion mismatch were the likely causes of the difference in phase transition temperatures between PLZT thin films and bulk ceramics.

A final observation of these thin-film results was that films on Pt/Si yielded higher T_Cs than films on silver. For example, the Curie temperature of the 9.5/65/35 film on Pt/Si was 30 °C higher than the same composition on silver and 15 °C higher than 7/65/35 on silver which should possess a much higher T_C than 9.5/65/35. Stress effects were the cause of these differences in phase transition temperatures. Because the PLZT films on Pt/Si were influenced by tensile stress, the thin-film material tended to remain in the larger-volume ferroelectric rhombohedral state with increasing temperature, while films on silver transformed to the paraelectric cubic phase at lower temperatures due to the influence of compressive stress which favoured the cubic phase with smaller unit cell volume.

3.5. Interfacial effects

Another major factor influencing thin-film properties is interface reaction between the ferroelectric film and

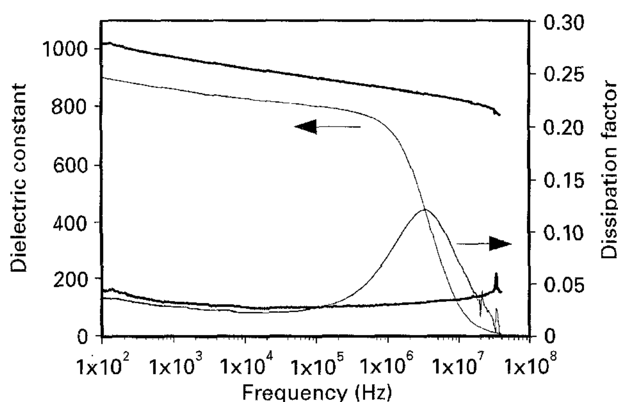

Figure 6 Dielectric relaxation behaviour of (—) a 2/55/45 thin film on Pt/Si compared with (—) a bulk ceramic showing a decrease in dielectric constant and peak in dissipation factor at the relaxation frequency for the thin film.

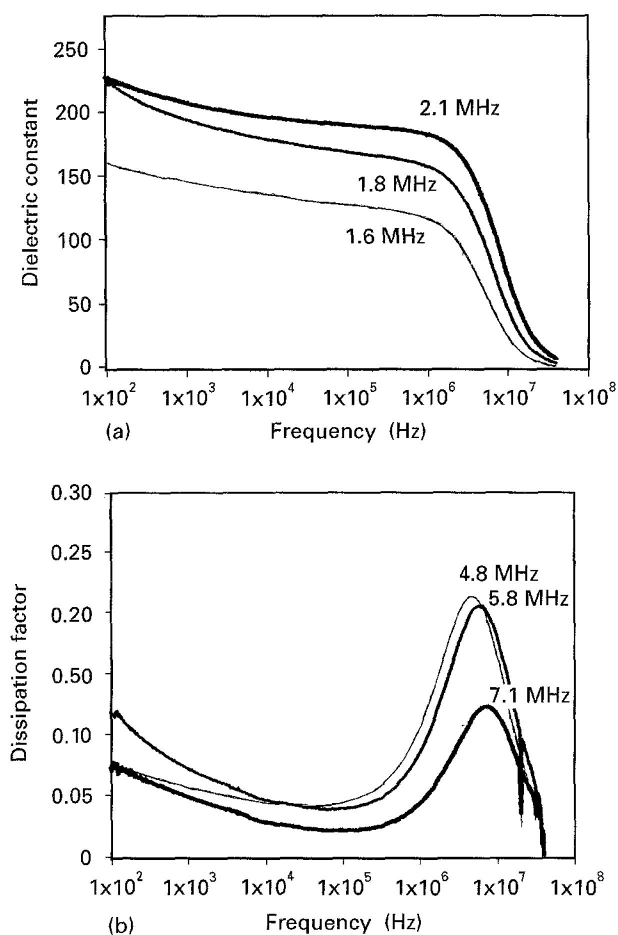

Figure 7 Dielectric relaxation behaviour of antiferroelectric 0/96/4 thin films on Pt/Si with variable thickness showing (a) decrease in dielectric constants and (b) the peak in dissipation factors at the relaxation frequencies. (—) 0.91 μm, (—) 0.49 μm, (—) 0.25 μm.

the underlying substrate and/or electrode during heat treatment. If stress was solely responsible for the differences between thin film and bulk ferroelectric properties, it may be expected that compressive stress would improve domain switching (i.e. increased P_R, decreased E_C) above normal bulk ferroelectric behaviour, while tensile stress would impede domain switching. Consequently, other factors such as finer microstructure and interfacial effects must, to a large extent, influence thin-film ferroelectric properties. A sharp decrease in dielectric constant near 1 MHz and a peak in dissipation factor at 3.3 MHz were observed for the PLZT 2/55/45 spin-coated thin film on Pt/Si shown in Fig. 6, while no such frequency dispersion occurred in the bulk 2/55/45. As indicated by the curve for the bulk material, however, the onset of the expected dielectric relaxation appeared imminent beyond 40 MHz as the dielectric constant began to decrease and the dissipation factor increased. Dielectric relaxation in bulk materials is expected to occur much later, at approximately 10^8–10^9 Hz, than for thin films [23]. This frequency dispersion of the dielectric constant, which can be caused by the loss of piezoelectricity and the clamping of domain walls [24], was probably shifted to lower frequency in the PLZT thin film due to clamping from the silicon substrate, low-K interface layer formation between the film and platinum, or increased platinum electrode resistance caused by interdiffusion with the PLZT during annealing.

Further evidence of interface reaction between PZT and platinum is shown in Fig. 7 for antiferroelectric PZT 0/96/4 thin films of various thickness spin-coated on Pt/Si. Dielectric constant characteristics revealed that the dielectric relaxation frequency decreased from 2.1 MHz to 1.6 MHz as film thickness was decreased from 0.91 μm to 0.25 μm. Accordingly, the peak in dissipation factor associated with the dielectric relaxation decreased from 7.1 MHz to 4.8 MHz with decreasing thickness. Because some reaction between the PZT and platinum during thermal processing at 700 °C was probable, the decrease in relaxation frequency may be attributed to an interface layer with low dielectric constant which increasingly influenced thin film properties with decreasing film thickness. It was also observed that the value of K decreased and the maximum $\tan\delta$ increased with decreasing film thickness.

Increased annealing time was also found to adversely influence the hysteresis properties of antiferroelectric lead zirconate 0/100/0 thin films. These antiferroelectric films were chosen for study because of their higher dielectric breakdown strength than conventional ferroelectric compositions. In Figs 8–10, the antiferroelectric double hysteresis loops of three lead zirconate films spin-coated on Pt/Si were obtained first at a moderate electric field level, i.e. 430–490 kV cm^{-1} (43–49 V μm^{-1}), then at an extremely high electric field of 710–740 kV cm^{-1} (71–74 V μm^{-1}) and, finally, again at the moderate field level. Fig. 8 displays a ten layer thin film heat treated at 700 °C for a total of 25 min, while Figs 9 and 10 show five layer films pyrolysed for 25 and 15 min, respectively. Both 25 min films exhibited hysteresis degradation after high-field application, as revealed by decreased sharpness of the antiferroelectric to ferroelectric transition and increased hysteresis loop asymmetry in Figs 8c and 9c; however, the five layer film degraded to a lesser extent than the ten layer film, indicating either a higher breakdown strength or an effect of the lower overall voltage applied to the thinner film. The hysteresis loop of the 15 min film in Fig. 10c showed no

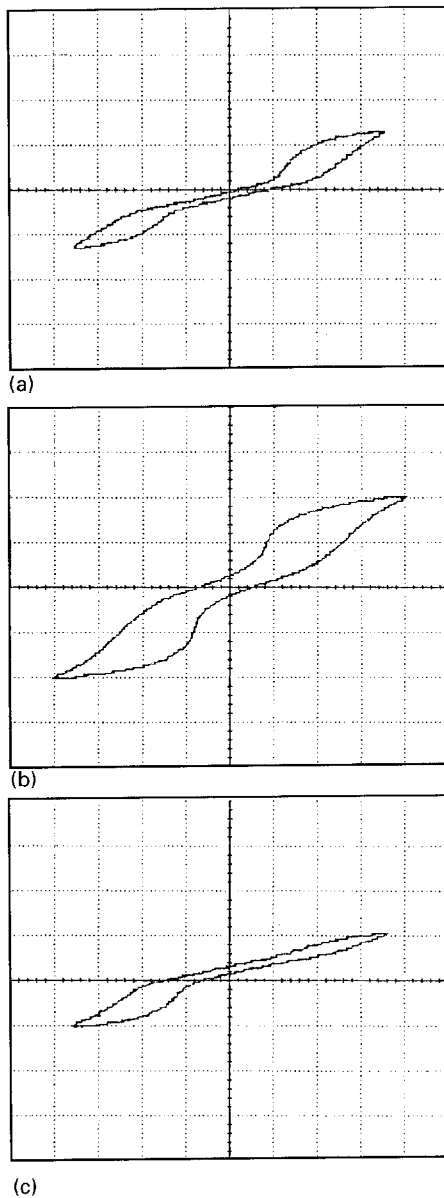

Figure 8 P–E hysteresis loops of an antiferroelectric 0/100/0 ten layer film with total annealing time of 25 min at 700 °C obtained at (a) 43 V μm^{-1}, (b) 71 V μm^{-1} and (c) again at 43 V μm^{-1} after high voltage was applied. The scale for the y-axis (polarization) is 15 μC cm^{-2} per division, and the x-axis (electric field) is 120 kV cm^{-1} per division for the low applied voltage and 180 kV cm^{-1} for high applied voltage conditions.

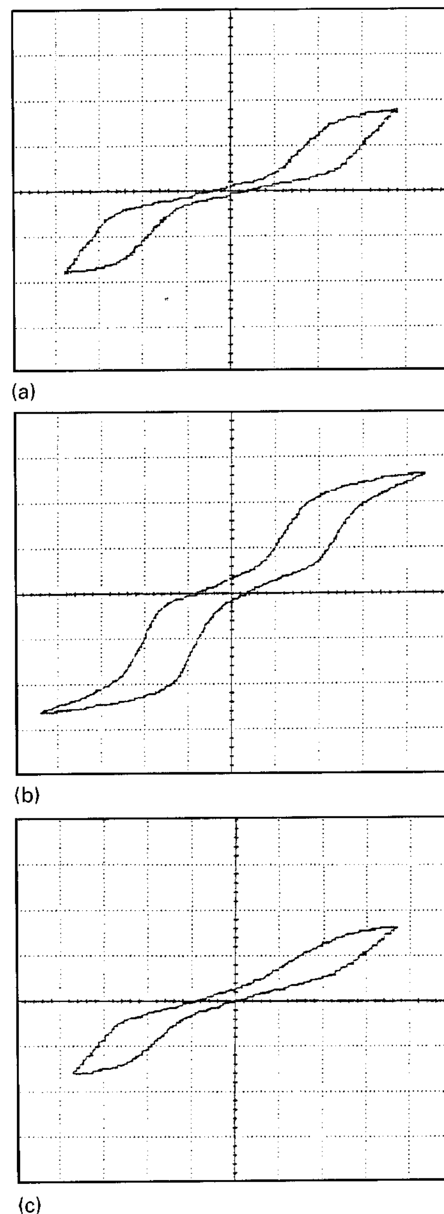

Figure 9 P–E hysteresis loops of an antiferroelectric 0/100/0 five layer film with total annealing time of 25 min at 700 °C obtained at (a) 43 V μm^{-1}, (b) 74 V μm^{-1} and (c) again at 43 V μm^{-1} after high voltage was applied. The scale for the y-axis (polarization) is 15 μC cm^{-2} per division, and the x-axis (electric field) is 120 kV cm^{-1} per division for the low applied voltage and 180 kV cm^{-1} for high applied voltage conditions.

evidence of degradation after the high-field application. Hence, the lower firing time potentially reduced interdiffusion or reaction at the film/platinum interface and yielded sharper field-induced transitions from the antiferroelectric antiparallel domain state to the ferroelectric parallel domain state both before and after the application of the high 73 V μm^{-1} electric field.

4. Conclusions

Chemically derived PLZT bulk ceramics and thin films were fabricated from the same acetate precursor solutions, and a number of physical and electrical properties were investigated in order to reveal similarities and differences between thin-film and bulk ceramic materials. The conclusions are as follows.

1. Internal stress was induced in thin-film materials due to thermal expansion mismatch with the underlying substrates. Films on Pt/Si exhibited a decrease in d-spacings normal to the substrate surface owing to two-dimensional tensile stress parallel to this surface; furthermore, films on silver with two-dimensional compressive stress possessed increased d-spacings normal to the substrate surface compared with the relatively stress-free bulk material. The grain size of the bulk material was also five times larger than for thin films.

2. Tensile stress caused preferential domain alignment perpendicular to the applied electric field, and compressive stress created domain alignment in the direction of this field. This produced impeded domain switching indicated by slanted, less-square hysteresis loops for films on Pt/Si, while bulk-like, square

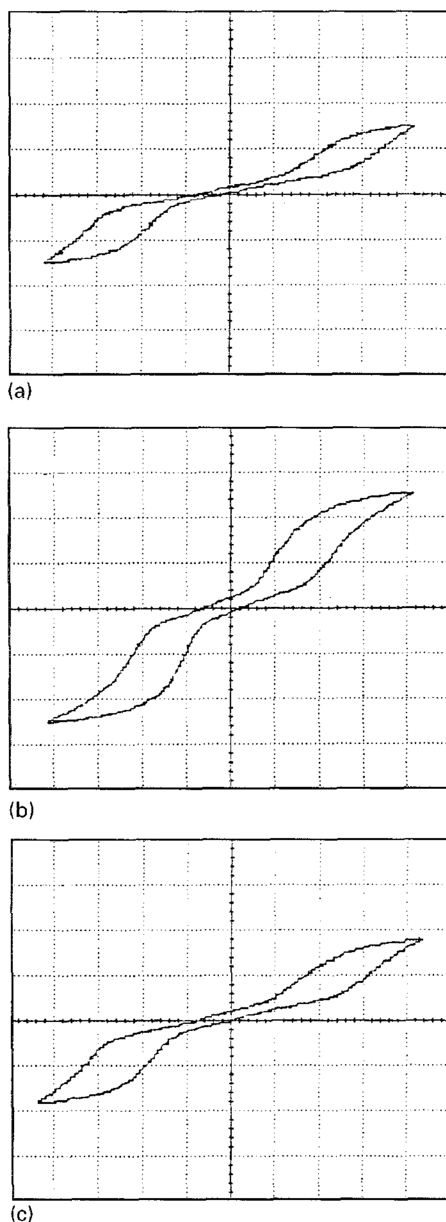

Figure 10 P–E hysteresis loops of an antiferroelectric 0/100/0 five layer film with total annealing time of 15 min at 700 °C obtained at (a) 49 V μm^{-1}, (b) 73 V μm^{-1} and (c) again at 49 V μm^{-1} after high voltage was applied. The scale for the y-axis (polarization) is 15 μC cm^{-2} per division, and the x-axis (electric field) is 120 kV cm^{-1} per division for the low applied voltage and 180 kV cm^{-1} for high applied voltage conditions.

hysteresis properties were observed in films on silver. E_C was higher and K was lower for all of the thin-film materials compared with the bulk.

3. Thin-film dielectric and hysteresis properties followed similar trends as bulk properties; however, the MPB was shifted slightly toward the lead zirconate end member for thin films on silver, indicating a more enhanced stability of the tetragonal phase. Compressive and tensile stress in thin films prevented these materials from exhibiting slim-loop ferroelectric behaviour as shown by the bulk material for x/65/35 with ⩾9% La due to enhanced polar region ordering in the films. T_Cs for x/65/35 thin films were higher than for bulk materials as a result of internal stress and smaller grain size, and films on Pt/Si exhibited higher T_Cs than films on silver, since tensile stress favoured the larger-volume ferroelectric phase near T_C.

4. Dielectric relaxation occurred for thin films near 1 MHz; however, this phenomenon was not observed in the bulk materials for the frequency range measured. Lower relaxation frequency was observed due to interface effects or piezoelectric clamping in the films from the substrate. Interface effects also became more pronounced with increased annealing time resulting in more degradation in antiferroelectric double hysteresis loops after a 73 V μm^{-1} electric field was applied.

Acknowledgments

Special thanks are extended to Dr Eugene Furman for his insightful viewpoints and valuable assistance. This work was supported by the Office of Naval Research under contract number N00014-91-J-1508.

References

1. G. H. HAERTLING, in “Ceramic Materials for Electronics”, 2nd Edn, edited by R. C. Buchanan (Marcel Dekker, New York, 1991) pp. 129–206.
2. G. GOODMAN, *ibid.*, pp. 69–128.
3. M. SAYER, in “Proceedings of the 3rd International Symposium on Integrated Ferroelectrics”, edited by C. A. Paz De Araujo (University of Colorado; Colorado Springs, USA, 1991) p. 1.
4. S. K. DEY, C. K. BARLINGAY, J. J. LEE, T. K. GLOERSTAD and C. T. A. SUCHICITAL, *ibid.*, p. 30.
5. L. M. SHEPPARD, *Am. Ceram. Soc. Bull.* **71** (1992) 85.
6. G. H. HAERTLING, *J. Vac. Sci. Technol. A* **9** (1991) 414.
7. Y. XU and J. D. MACKENZIE, *Integ. Ferroelect.* **1** (1992) 17.
8. K. D. BUDD, S. K. DEY and D. A. PAYNE, *Br. Ceram. Proc.* **36** (1985) 107.
9. G. H. HAERTLING, in “Proceedings of the 7th IEEE, International Symposium on Applications of Ferroelectrics” edited by S. B. Krupanidhi and S. K. Kurtz (IEEE; New York, USA, 1990) p. 292.
10. H. WATANABE, T. MIHARA and C. A. PAZ DE ARAUJO, in “Proceedings of the 3rd International Symposium on Integrated Ferroelectrics”, edited by C. A. Paz De Araujo (University of Colorado; Colorado Springs, USA, 1991) p. 139.
11. D. R. LIDE (ed.), “Handbook of Chemistry and Physics”, 71st Edn (CRC Press, Boca Raton, 1990).
12. K. K. LI, PhD dissertation, Clemson University, Clemson, SC (1993).
13. D. E. DAUSCH, PhD dissertation, Clemson University, Clemson, SC (1995).
14. G. H. HAERTLING, in “Engineered Materials Handbook”, Vol. 4, “Ceramics and Glasses”, edited by S. R. Lampman, M. S. Woods and T. B. Zorc (ASM International, Metals Park, Ohio, USA, 1991) pp. 1124–30.
15. L. SHI, S. B. KRUPANIDHI and G. H. HAERTLING, *Integ. Ferroelect.* **1** (1992) 111.
16. G. H. HAERTLING, *Ferroelectrics* **116** (1991) 51.
17. *Idem, Integ. Ferroelect.* **3** (1993) 207.
18. W. Y. GU, E. FURMAN, A. BHALLA and L. E. CROSS, *Ferroelectrics* **89** (1989) 221.
19. G. A. ROSSETTI Jr, L. E. CROSS and K. KUSHIDA, *Appl. Phys. Lett.* **59** (1991) 2524.
20. E. SVIRIDOV, V. ALYOSHIN, Y. GOLOVKO, I. ZAKHARCHENKO, V. MUKHORTOV and V. DUDKEVICH, *Ferroelectrics* **128** (1992) 1.
21. R. W. VEST and J. XU, *ibid.* **93** (1989) 21.
22. K. OKAZAKI and K. NAGATA, *J. Am. Ceram. Soc.* **56** (1973) 82.
23. M. SAYER, A. MANSINGH, A. K. ARORA and A. LO, *Integ. Ferroelectr.* **1** (1992) 129.
24. J. CHEN, K. R. UDAYAKUMAR, K. G. BROOKS and L. E. CROSS, *J. Appl. Phys.* **71** (1992) 4465.

Received 20 September 1995
and accepted 15 January 1996